

Compositional variation of AlGa_xN epitaxial films on 6H-SiC substrates determined by cathodoluminescence.

A. Petersson^{1,4}, Anders Gustafsson¹, L. Samuelson¹, Satoru Tanaka² and Yoshinobu Aoyagi³

¹Division of Solid State Physics, Lund University, Box 118, S-221 00 Lund, Sweden,

²Research Institute for Electronic Science, Hokkaido University, Kita, 12-Nishi 6, Kita-ku, Sapporo 060-0812 Japan,

³The Institute of Physical and Chemical Research (RIKEN),

⁴Crystal Fibre A/S, Blokken 84, DK-3460 Birkerød, Denmark,

(Received Friday, May 3, 2002; accepted Thursday, June 27, 2002)

High quality epitaxial films of Al_xGa_{1-x}N, grown on SiC substrates, were investigated using spatially resolved cathodoluminescence (CL), scanning electron microscopy, and atomic force microscopy. A variation in the observed peak energy position of the CL was related to alloy fluctuations. CL was used to reveal relative alloy fluctuations of approximately 1% on a sub-micrometer scale, with a precision difficult to surpass with other available techniques. By correlating data from the different techniques, a model was derived. The main feature of it is an alloy fluctuation on the micrometer scale, seeded during the initial growth and extending through the epitaxial film. These alloy fluctuations seems to be related to terrace steps (≈ 5 nm in height), formed preferentially at scratches on the SiC surface. This investigation indicates that the initial growth of epitaxial films is critical and structures formed at the beginning of the growth tend to persist throughout the growth. Further, a strain gradient from the SiC interface extending towards the surface, was observed.

1 Introduction

III-V nitrides, and especially the ternary compounds of AlGa_xN, are technologically important for the fabrication of light emitting diodes and laser diodes emitting light in the blue and UV region [1]. These compounds are also important for the development and fabrication of high power and high frequency devices [2]. AlGa_xN is generally used as the barrier material for GaN or GaInN quantum structures, mainly quantum wells. One of the most serious problems concerning the epitaxial growth of high quality AlGa_xN epitaxially on substrates of sapphire and SiC, is the large lattice mismatch and the differences in thermal expansion coefficients between the substrate and the AlGa_xN film. These unfavorable conditions for growth make it difficult to obtain high quality AlGa_xN films and it is essential to develop an understanding of the factors that are crucial for obtaining a high crystal quality.

In this investigation, the structural and optical properties of AlGa_xN epitaxial films were studied. Spatially resolved, scanning electron microscopy (SEM)-based cathodoluminescence (CL) at low temperatures (15-80K), was used to investigate the quality of the epitaxial

film. This was done in both top view and cross-section. CL is one of the most powerful methods for characterizing small alloy fluctuations in AlGa_xN films, on a sub-micrometer scale, with a precision difficult to surpass with any other available technique. This makes CL an important diagnostic tool in the development of high quality AlGa_xN epitaxial films. The epitaxial films were also investigated using atomic force microscopy (AFM), transmission electron microscopy (TEM) and field emission scanning electron microscopy (FSEM).

The geometrical structure of epitaxial films is usually determined by methods such as SEM, TEM, AFM, and scanning tunneling microscopy (STM). Variations in the composition of an epitaxial film can, to some extent, be determined by SEM, TEM and STM, but to acquire more detail about the composition, methods such as X-ray diffraction spectroscopy, energy dispersive X-ray analysis, Auger spectroscopy, secondary ion mass spectroscopy and particle induced X-ray emission must be used. In this work, the high spatial resolution of CL and variations in the peak energy position of the luminescence were used to show variations in the composition of the epitaxial films. It would be difficult, if

not impossible, to simultaneously study the spatial variations in composition with the same level of precision using any other method. Spectrally resolved luminescence is a sensitive probe of the $\text{Al}_x\text{Ga}_{1-x}\text{N}$ composition; a variation of 0.01 in x gives a shift in energy of ≈ 28 meV, with an increase in the Al content giving an increase in the position of the emission energy. However, this method must be used with the greatest care, since the AlGa N composition is not the only parameter that alters the peak energy position of the luminescence of an AlGa N layer. The energy position may also be influenced by crystal polytypes, strain, the presence of impurities, sample temperature, quantum effects and excitation density. To justify the interpretation of the results obtained by CL, the effects of the other potential sources must be accounted for. It is worth pointing out that there are two origins of the strain in an AlGa N layer on SiC [3]. One is from the actual lattice mismatch between the substrate and the epitaxial film, which introduces an in-plane compressive strain in the epitaxial film. The second component is from the significant difference in thermal expansion of the two. This introduces an additional in-plane tensile strain as the sample is cooled down from the growth temperature. It is generally considered that the epitaxial film will relax during growth, and the major strain in the films at room temperature is related to differences in the thermal expansion. As an example, tensile strain has been reported to introduce shifts from ≈ 4 meV [4] [5] to ≈ 16 meV [6], in the case of Ga N . The factors contributing to the full width at half maximum (FWHM) of the luminescence from the present AlGa N films were investigated, and it will be shown below that a significant contribution can be attributed to alloy fluctuations on a micrometer scale.

2 Growth

The samples in this work were grown in a conventional horizontal-type, low-pressure metal organic chemical vapor deposition system on the Si face of on-axis 6H-SiC (0001), using a growth temperature of 1080°C and the precursors TMAI, TMGa and NH_3 . The structure was fabricated by starting at the SiC interface with a 1-3 nm thick AlN buffer layer, followed by a 0.5 μm thick $\text{Al}_{0.12}\text{Ga}_{0.88}\text{N}$ layer. The layers are nominally undoped, but there can be a significant unintentional Si doping originating from the substrate [7]. Details of the growth can be found elsewhere [8].

3 Structural Properties

To study the structure of the epitaxial films on a large scale, we investigated the samples in top view and cross section using high resolution FSEM. In this study, the experimental spatial resolution was better than 10 nm. Images recorded in top-view (not shown here) displayed

no features, indicating a smooth surface and, therefore, a uniform film, on the SEM scale. The SEM images of the cleaved sample were recorded with the sample tilted ≈ 30 degrees away from the growth direction. SEM images recorded from the cleaved edge of a sample, as shown in figure 1, also display a uniform film on the 10 nm scale. The thickness of the film was found to be ≈ 700 nm. No SEM images recorded normal to the cleaved plane are shown, since the secondary electron signal from the edge of the sample was very strong. This large variation in intensity over the image makes interpretation of such images difficult.

The surface of a 6H-SiC substrate was characterized by AFM, in order to investigate the possible influence of surface morphology on the subsequent epitaxial growth. This study revealed the presence of what appears to be scratches on the surface of the substrate. An AFM image of a typical substrate surface is presented in figure 2. The scratches, originating from mechanical polishing of the surface, display a characteristic pattern. The width of the scratches is typically ≈ 500 nm and the depth is as large as 30 nm. The scratches are randomly oriented, which leads us to exclude that they are growth-related structures or defects in the substrate. They would be related to certain crystallographic directions, rather than being randomly distributed, as in the AFM images. Between the scratches, the SiC surface is flat within the resolution of the AFM.

AFM measurements of the surface of a typical epitaxial AlGa N film reveal two types of patterns, figure 3. First, the surface displays a terrace-like structure, with a typical width of ≈ 2000 nm and a typical step height of ≈ 5 nm. This structure is typical for III-nitrides and is referred to as mosaic or columnar structure [9]. Assuming atomically flat terraces, this implies a tilt of the entire film in the order of 0.2 degrees away from the [0 0 0 1] growth direction. This could be related either to substrate tilt or a tilt induced by strain relaxation. Second, a comparison of the AFM images of figure 2 and figure 3 shows that a pattern similar to that of the deep scratches, observed on the surface of the SiC substrate (figure 2), was also present on the surface of the epitaxial film (figure 3). In the epitaxial film, the pattern is present in the form of slightly higher terrace steps (≈ 10 nm in height). It is somewhat surprising that the pattern is still visible after 700 nm of growth.

Epitaxial films grown under similar conditions were investigated by TEM (not shown here). High resolution TEM micrographs, as well as the TEM diffraction patterns, displayed only the wurtzite structure of the AlGa N in these films. The TEM investigations revealed that the AlGa N film grew with the c -axis perpendicular to the growth direction, as expected. Furthermore, no micro-racks were observed in the TEM study.

4 Optical Properties

The CL data in this study was obtained at low temperature, generally 15–20 K, and at low acceleration voltages of 3–5 kV. A typical, spatially averaged (from a region of 20 by 20 μm^2) luminescence spectrum is shown in figure 4. An acceleration voltage of 3 kV was used, giving a penetration depth (Grün range) of 100 nm [10]. Assuming a very short diffusion length (<100 nm in GaN [11]) of the generated carriers in the AlGaIn film, the major part of the observed luminescence originates from the top 100 nm of the film. The main peak at 3.723 eV, denoted "AlGaIn", is attributed to the recombination of excitons in the epitaxial film [12]. On the low-energy side of the main peak, there is a less intense peak, denoted "LO1". The energy of this peak is ≈ 90 meV lower than that of the main peak and is assumed to be the first phonon replica (longitudinal optical phonon) of the main peak. The weaker peaks; "LO2" and "LO3" are believed to be the second and third phonon replicas, respectively. The FWHM of the excitonic peak in figure 4 is 34 meV, which is comparable with what has been reported [13] [14]. It was also found that the spatial distribution of the luminescence intensity was rather uniform. This was determined using monochromatic CL images, recorded at the peak energy position of the excitonic luminescence. In these images, the smallest features that can be resolved are ≈ 250 nm in size. This seems to indicate that the film is uniform and the width of the luminescence peak is related to variations on a scale smaller than 250 nm. However, more detailed investigations reveal that the AlGaIn epitaxial films have a more complex structure. In the remainder of this article, measurements showing different aspects of the structure of the films will be presented.

The spatial distribution of the luminescence from the sample was investigated by recording a series of CL images at different emission energies. Three of these images are presented in figure 5. The used acceleration voltage of 5 kV mainly probes the top 250 nm, as discussed above. The first CL image, figure 5(b), was recorded at 3.72 eV, corresponding to the peak position of the main luminescence peak. The intensity variations on a large spatial scale observed in this image are caused by spatial variations in the efficiency of the detection system used here, and are common to all CL images recorded at this low magnification. The weak intensity variations, on a small spatial scale, give the impression that the luminescence from the epitaxial film is highly uniform. But this is only true for images recorded at the peak energy position. For images recorded at a higher energy, 3.74 eV (figure 5(c)), and a lower energy, 3.70 eV (figure 5(a)), this is no longer true. The most striking features observed in figure 5(a) and (c) are the bright/

dark lines in the images. The two images show complementary contrast variations, where a bright line in one image is dark in the other, and vice versa. This behavior indicates variations in the peak energy position of the luminescence. We will tentatively attribute this to a spatial variation of the bandgap of the AlGaIn. Furthermore, the pattern of lines resembles the pattern of the scratches from the mechanical polishing, previously observed in the AFM image, figure 2, of the surface of the SiC substrate. As discussed above, the same type of pattern can be found on the surface of the epitaxial film as well, figure 3. This type of pattern indicates that the bandgap variations could be related to terrace steps on the surface of the film. The comparison above of the AFM images of the substrate and of the film, indicates a relation between the surface structures. This suggests that the bandgap variations, related to the surface structures, extend through the entire thickness of the film. This point will be addressed in a later section. There has been a report of scratches influencing the optical properties of AlGaIn films [15]. However, these were large enough to be observed in the SEM during the CL measurements, and the only effect they had was to lower the signal emission from the scratched area.

An interesting observation is that, in contrast to what is normally observed, the low energy CL image (figure 5(a)) displays sharper features than the high energy CL image (figure 5(b)). The finer features in CL images of the low-bandgap luminescence are often blurred by the diffusion of carriers from the surrounding high-bandgap material. The sharp features observed for the low-energy image are a further indication of the short diffusion length of the material, as discussed above. These features can also be caused by a region of low-energy material surrounded by thin layers of high energy material, preventing diffusion into the low-energy regions. In both cases, these sharp features suggest that the regions of low-bandgap material are smaller than their apparent size in the images.

Further evidence that the low-bandgap regions are small is given by the dependence of the luminescence on the probe current (the excitation density). By varying the electron beam current in the CL system, the excitation-density dependence of the luminescence from the epitaxial film can be probed. In figure 6, it was found that the FWHM of the luminescence peak decreased with increasing excitation density. By increasing the probe current by a factor of 50, the FWHM was decreased from 34 meV to 28 meV. One interpretation of the spectral sharpening is that the low-bandgap volumes are so small that they easily get saturated, and as the excitation density increases, the dominance of the luminescence from the high bandgap regions is even more pronounced.

A more detailed investigation of the luminescence variations can be performed by recording a series of CL spectra at points along a line on the sample. In figure 7 such a line scan is presented. The left side of the figure is an intensity plot of the CL along a randomly oriented line. The x and y axes in the intensity plot correspond to the emission energy and the spatial position along the line, respectively. The brightness of each pixel corresponds to the intensity recorded at that point (energy and spatial position). In order to enhance perception of the energy-position variations, contour curves are included in the image. On the right-hand side of figure 7, the individual CL spectra from points indicated by the connecting lines are presented.

An inspection of the line scan in figure 7 shows that the peak energy position of the luminescence varies along the line. This implies that the intensity variations observed in monochromatic CL images (figure 5 (a) and (c)) are mainly related to shifts in the peak energy position and not to variations in total intensity. This is corroborated by the complementary behavior of the high and low energy images of figure 5 (a) and (c). The FWHM of the local luminescence, as shown in the right side of figure 7, is narrower than the FWHM of the peak formed by averaging the luminescence from a large region, figure 4. This clearly shows that a large portion of the FWHM can be attributed to local variations in the peak position. Furthermore, the peak energy position exhibits discrete jumps with variations in spatial position, rather than a continuous variation. However, the individual peak energy positions seem to be randomly scattered over a range of ≈ 25 meV, where the discrete jumps could be related to differences in the luminescence of the individual terraces and steps along the line scan.

The structure along the growth direction can, in principle, be studied in top view, by varying the acceleration voltage of the CL-SEM, and thereby the penetration depth. By changing from 3 to 30 kV, the penetration depth changes from ≈ 100 nm to ≈ 4000 nm. However, with an unclear excitation-density dependence, artifacts may be introduced by variations in the depth profile of the excitation density. In addition, as a first estimate, the minimum feature size observed in CL increases linearly with penetration depth, due to the larger in-plane scattering of the electrons. To avoid these difficulties in the interpretation of the data, the vertical structure of the film was investigated by recording cross-sectional CL images of the side of a cleaved sample, as shown in figure 8. As before, the cleaved sample was mounted at an angle, in this case ≈ 45 degrees, to avoid the edge effects in the SEM images, as discussed above. The CL images were recorded at 3.69 eV (figure 8 (a)) and 3.75 eV (figure (b)). By comparing the two images, it was found that

the high-energy luminescence dominated close to the SiC interface, whereas the low-energy luminescence dominated near the surface of the epitaxial film. This indicates a gradient in the bandgap, high at the SiC interface and decreasing towards the surface. A possible explanation for this behavior can be found by comparing this result with a study of a ≈ 200 μm thick epitaxial layer of GaN, grown on a sapphire substrate [16] [17]. Due to the smaller lattice constant of sapphire, the GaN is expected to grow under compressive strain. Most of this strain relaxes by the formation of dislocations during the initial growth [18], and the major part of a thick film is virtually strain free at the growth temperature. In contrast, *in-situ* measurements of the strain has shown that GaN on a low-temperature AlN buffer layer grows under *tension* and that no relaxation takes place in films up to several μm of thickness [19]. However, due to the smaller thermal expansion coefficient of GaN compared with sapphire (the sapphire substrate shrinks faster than the GaN), additional compressive strain is introduced in the film as the layer cools down to room temperature. This strain is relaxed starting from the surface, which means that there is some residual compressive strain in the film near the sapphire interface. This increases the bandgap of the GaN at the interface.

In the case of (Al)GaN on SiC, the lattice constant of SiC is also smaller and the film will initially grow under compressive strain. As in the case of sapphire substrates, this strain is gradually relaxed by the introduction of dislocations as the layer grows thicker. As the structure cools down to room temperature, the epitaxial film shrinks faster than the substrate, which introduces an additional tensile strain. At room temperature and at liquid helium temperature, there is therefore a strain gradient, with decreasing compressive strain towards the surface of the film. If the film is thick enough, the strain can change to tensile towards the surface. There is a discussion in the literature about whether the initial relaxation occurs over a few nm [18] or is more gradual [3]. It has been shown that thicker layers ($> 3\mu\text{m}$) of GaN on SiC are usually under tensile strain [4] [5], whereas thinner layers ($< 0.7\mu\text{m}$) are under compressive strain [3] [6]. In addition, the compressive strain introduces an increase in the bandgap and the tensile strain introduces a decrease in the bandgap of AlGaIn [4] [5]. In the sample shown in figure 8, there is a gradient in the bandgap, higher at the interface and lower at the surface. According to the discussion above, this indicates a decreasing compressive strain (or increasing tensile strain) with distance from the interface in the present sample.

CL images were recorded under the same conditions as the images of figure 8, varying the detected photon energy. In the case of figure 9, the energy was 3.66 eV, below the energy of the emission from the compressive

sively strained region of the AlGa_xN film. With the present geometry of sample mounting, it is possible to simultaneously obtain cross-sectional, as well as, top view information, yielding semi three-dimensional information. The CL image, in figure 9, displays an interesting feature, a bright region indicated by the arrow on the left. This region extends straight from the SiC interface through the film to the surface, where it appears to continue along the surface in a random fashion, suggesting that this region is a vertical sheet of low-bandgap material.

5 Discussion

The most probable cause of the regions emitting low-energy luminescence is a variation in composition, where these regions are Ga-rich. In order to justify this assumption, it has to be established that the main cause of the low-bandgap regions can be attributed to variations in the Ga-to-Al ratio in the AlGa_xN films. (i) The TEM investigation indicates that only the wurtzite polytype is present, excluding different polytypes (e.g. cubic AlGa_xN) as a source of the variations in the bandgap. (ii) We observe a gradient in the strain in the vertical direction of the film, as shown in figure 8. This is due to the lattice mismatch and the difference in thermal expansion coefficients of the SiC substrate and the AlGa_xN film. (iii) The variations in peak energy position, related to the lateral patterns observed in the CL images of figure 5 (a) and (c), penetrate the film vertically, as shown in figure 9. It is very unlikely that local variations in strain (i.e., inhomogeneous strain relaxation) would produce these structures that penetrate the entire film. Local variations in the strain could be introduced by alloy fluctuations, in which case these would still be the origin of the fluctuations in the energy position. (iv) Microcracks can introduce local relaxation of the film, and give rise to the type of patterns we observe [20]. However, neither the TEM nor the SEM investigation revealed any microcracks in the present films. (v) Segregation of impurities to grain boundaries have been shown to introduce line patterns in GaN films [21]. In this reference 20, the energy difference was 2–300 meV and the impurity was an acceptor. It is unlikely that the variations are caused by luminescence from impurities, since we observe a scatter over 25 meV in the peak energy position in the line scan in figure 7. If the variations were related to the presence of impurities, a discrete energy shift related to the impurity would be expected. Several different peak positions, as observed in figure 7, would require different impurities. (vi) Quantum effects can also be dismissed, since these require a variation in the bandgap to start with. In addition, quantum effects would increase the energy levels if the low bandgap regions were sufficiently small. This would lead to an

underestimation of compositional variations. In conclusion, the observed local variations in the peak energy position of the luminescence are most probably caused by local variations in the Al-to-Ga ratio in the Al_xGa_{1-x}N film. The extent of these variations is on scale of ± 0.005 .

There have been some reports on local deviation of the Al content during growth of AlGa_xN. The variations are mainly related to different facets introduced by growth defects. The facets have been either the funnels of nanopipes [22] or V-shaped defects connected to inversion domains [23]. However, in both cases, the Al content is *increased* on the additional facets. For growth on the non-planar substrates used in hetero-epitaxial lateral overgrowth, there can be a difference in Al incorporation between the terraces and the trenches. AlGa_xN, grown on 5 μm wide and 1 μm deep trenches exhibits a higher Ga content in the trenches than on the terraces [24] [25]. Dislocations, especially edge dislocations, can also be a source of an increase in Al incorporation [26] in AlGa_xN.

6 A Model for the compositional variations

At this stage, we will introduce a model for the structure of epitaxial films. This model is shown in figure 10, and the epitaxial films consists of a thick wurtzite AlGa_xN epitaxial film grown on a 6H-SiC (0001) substrate, which is nominally exactly oriented and flat. The AlGa_xN grows with the c-axis perpendicular to the surface of the SiC. The epitaxial film has a terrace-like structure, where the width of the terrace is ≈ 2000 nm and the height of the steps is ≈ 5 nm, indicating a local tilt of 0.2 degrees. The steps are, in general, randomly distributed (spacing and directions) on the surface. However, they can be preferentially formed in conjunction with scratches on the substrate surface. These scratches are produced during the mechanical polishing of the substrate. Due to differences in the surface mobility of the Al and the Ga species, the incorporation of Ga is enhanced at the steps, and narrow, Ga-rich regions are formed at the steps during growth. While the steps remain on the growing surface, these regions extend vertically. We believe that this is similar to the formation of vertical QWs and vertical quantum wires in the AlGaAs system [27] [28].

7 Summary

Epitaxial films of Al_xGa_{1-x}N ($x \approx 0.12$) were investigated, mainly using spatially resolved cathodoluminescence. The films were found to have a strain gradient, with decreasing compressive strain from the substrate interface to the surface. This gradient is believed to originate in a gradual relaxation of the initial compressive strain, as the films grew thicker, in combination with a

general tensile strain, introduced as the film cools down from the growth temperature. Spatial variations, on a sub-micrometer scale, in the luminescence in the plane of the epitaxial film were suggested to originate in variations in the composition, on a scale of $x \pm 0.005$. These variations seem to stem from the surface of the substrate, where Ga-rich (low bandgap) material is preferentially formed at scratches on the substrate surface. The Ga-rich regions extend through the epitaxial film, in the growth direction. In addition, we have demonstrated the power of the CL technique as a tool for studying compositional variations on a sub-micrometer scale.

REFERENCES

- [1] S. Nakamura, *Mater. Res. Bull.* **23**, 37 (1998).
- [2] M. Asif Khan, J. N. Kuznia, D. T. Olson, R. Kaplan, *J. Appl. Phys.* **73**, 3108-3110 (1993).
- [3] W.G. Perry, T. Zheleva, M.D. Bremser, R.F. Davis, W. Shan, J.J. Song, *J. Electron. Mater.* **26**, 224-231 (1997).
- [4] W. Shan, R.J. Hauenstein, A.J. Fischer, J.J. Song, W.G. Perry, M.D. Bremser, R.F. Davis, B. Goldenberg, *Phys. Rev. B* **54**, 13460 (1996).
- [5] W. Shan, A.J. Fischer, S.J. Hwang, B.D. Little, R.J. Hauenstein, X.C. Xie, J.J. Song, D.S. Kim, B. Goldenberg, R. Horning, S. Krishnankutty, W.G. Perry, M.D. Bremser, R.F. Davis, *J. Appl. Phys.* **83**, 455 (1998).
- [6] N.V. Edwards, M.D. Bremser, R.F. Davis, A.D. Batchelor, S.D. Yoo, C.F. Karan, D.E. Aspnes, *Appl. Phys. Lett.* **73**, 2808 (1998).
- [7] G. Popovici, W. Kim, A. Botchkarev, H. Tang, H. Morkoccedil, *Appl. Phys. Lett.* **71**, 3385 (1997).
- [8] S. Tanaka, S. Iwai, Y. Aoyagi, *J. Cryst. Growth* **170**, 329-334 (1997).
- [9] F. A. Ponce, *MRS Bull.* **22**, 51-57 (1997).
- [10] J.I. Goldstein, D.E. Newbury, P. Echlin, D.C. Joy, A.D. Romig, C.E. Lyman, C. Fiori, E. Lifshin, *Scanning Electron Microscopy and X-Ray Microanalysis*, (Plenum Press, New York, 1992), .
- [11] Shigefusa Chichibu, Kazumi Wada, Shuji Nakamura, *Appl. Phys. Lett.* **71**, 2346-2348 (1997).
- [12] B. Monemar, *Phys. Rev. B* **10**, 676 (1974).
- [13] M. D. Bremser, W. G. Perry, T. Zheleva, N. V. Edwards, O. H. Nam, N. Parikh, D. E. Aspnes, Robert F. Davis, *MRS Internet J. Nitride Semicond. Res.* **1**, 8 (1996).
- [14] W. Shan, A.J. Fischer, J.J. Song, G.E. Bulman, H.S. Kong, M.T. Leonard, W.G. Perry, M.D. Bremser, R.F. Davis, *Appl. Phys. Lett.* **69**, 740-742 (1996).
- [15] G. Steude, T. Christmann, B.K. Meyer, A. Goeldner, A. Hoffmann, F. Bertram, J. Christen, H. Amano, I. Akasaki, *MRS Internet J. Nitride Semicond. Res.* **4S1**, G3.26 (1999).
- [16] A. Hoffmann, J. Christen, H. Siegle, F. Bertram, D. Schmidt, L. Eckey, C. Thomsen, K. Hiramatsu, *Mater. Sci. Eng. B* **50**, 192 (1997).
- [17] H. Siegle, A. Hoffman, L. Eckey, C. Thomsen, J. Christen, F. Bertram, D. Schmidt, D. Rudloff, K. Hiramatsu, *Appl. Phys. Lett.* **71**, 2490 (1997).
- [18] K. Hiramatsu, T. Detchprohm, J. Akasaki, *Jpn. J. Appl. Phys.* **32**, 1528 (1993).
- [19] S. Hearne, E. Chason, J. Han, J. A. Floro, J. Figiel, J. Hunter, H. Amano, I. S. T. Tsong, *Appl. Phys. Lett.* **74**, 356 (1999).
- [20] C.E. Norman, R.A. Hogg, A.J. Shields, N. Iizuka, *Phys. Stat. Sol. B* **216**, 375 (1999).
- [21] Carol Trager-Cowan, P. G. Middleton, K. P. O'Donnell, S. Ruffenach-Clur, Olivier Briot, *MRS Internet J. Nitride Semicond. Res.* **2**, 31 (1997).
- [22] J. Kang, S. Tsunekawa, B. Shen, Z. Mai, C. Wang, T. Tsuru, A. Kasuya, *J. Cryst. Growth* **229**, 58 (2001).
- [23] B. Pecz, Zs. Makkai, M.A. di Forte-Poisson, F. Huet, R.E. Dunin-Borkowski, *Appl. Phys. Lett.* **78**, 1529 (2001).
- [24] M. Iwaya, S. Terao, T. Sano, T. Ukai, R. Nakamura, S. Kamiyama, H. Amano, I. Akasaki, *J. Cryst. Growth* **237-9**, 951-5 (2002).
- [25] T. Riemann, J. Christen, A. Kaschner, A. Laades, A. Hoffmann, C. Thomsen, M. Iwaya, S. Kamiyama, H. Amano, I. Akasaki, *Appl. Phys. Lett.* **80**, 3093 (2002).
- [26] L. Chang, S.K. Lai, F.R. Chen, J.J. Kai, *Appl. Phys. Lett.* **79**, 928 (2001).
- [27] A. Hartmann, L. Loubies, F. Reinhardt, E. Kapon, *Appl. Phys. Lett.* **71**, 1314 (1997).
- [28] E. Martinet, A. Gustafsson, G. Biasiol, F. Reinhardt, E. Kapon, K. Leifer, *Phys. Rev. B* **56**, R7093 (1997).

FIGURES

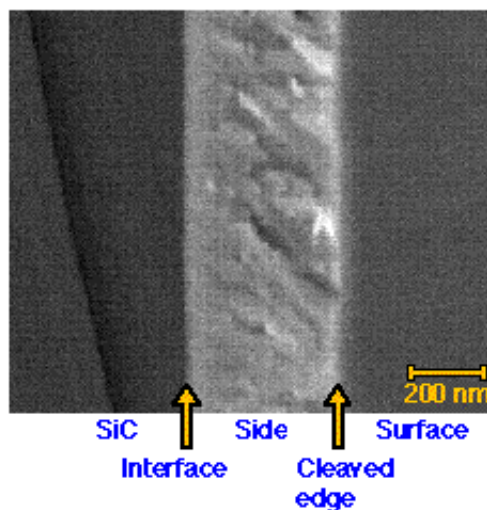


Figure 1. FSEM image of the cleaved edge of the epitaxial film.

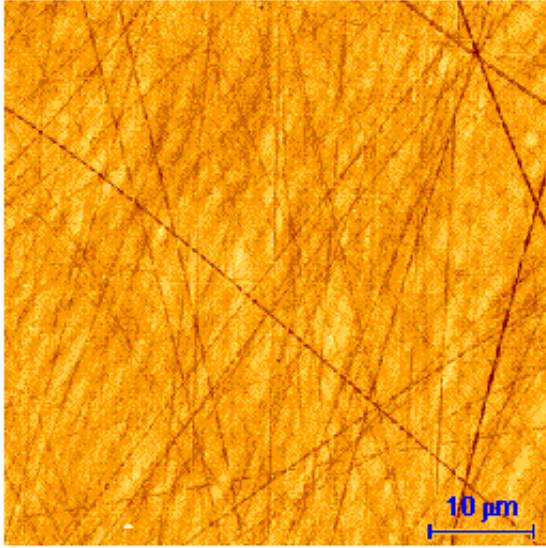


Figure 2. AFM image of the surface of a 6H-SiC substrate. The image reveals scratches on the surface, resulting from mechanical polishing.

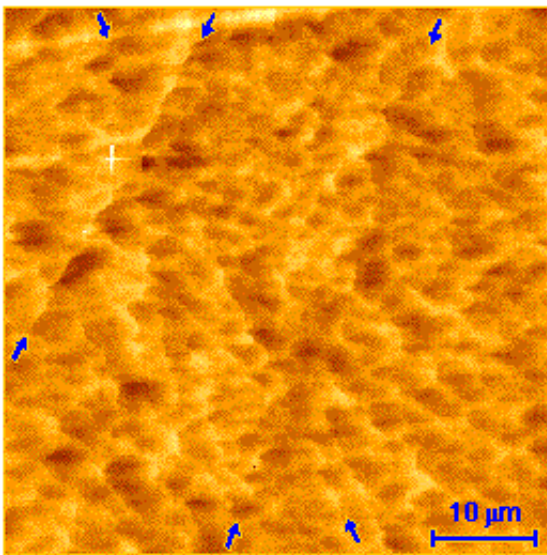


Figure 3. AFM image of the surface of an AlGaIn epitaxial layer. The arrows indicate structures assumed to originate from scratches on the surface of the substrate.

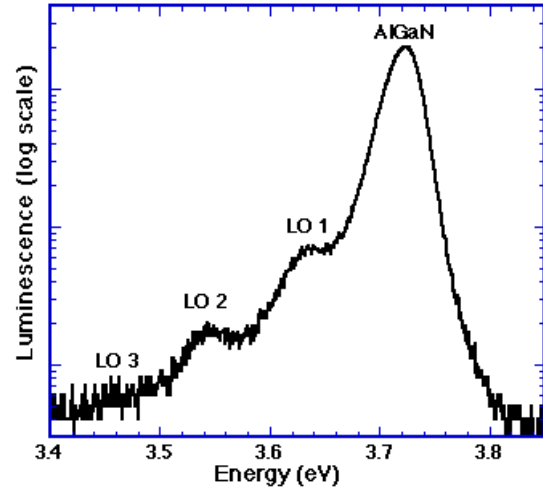


Figure 4. Spatially averaged spectrum of an AlGaIn epitaxial film.

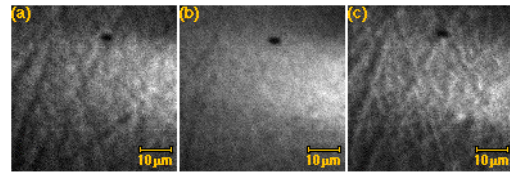


Figure 5. Monochromatic, top view CL images recorded at 30 K, using a 5 kV acceleration voltage. The images were recorded with the detection at (a) 3.70 eV, (b) 3.72 eV and (c) 3.74 eV, where (b) corresponds to the peak energy position of the excitonic emission from the film.

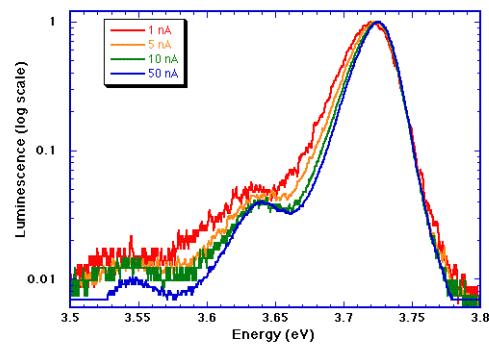


Figure 6. Spatially averaged cathodoluminescence spectra of an AlGaIn epitaxial film. The excitation density dependence is recorded by varying the electron beam current from 1 nA to 50 nA. The spectra are normalised.

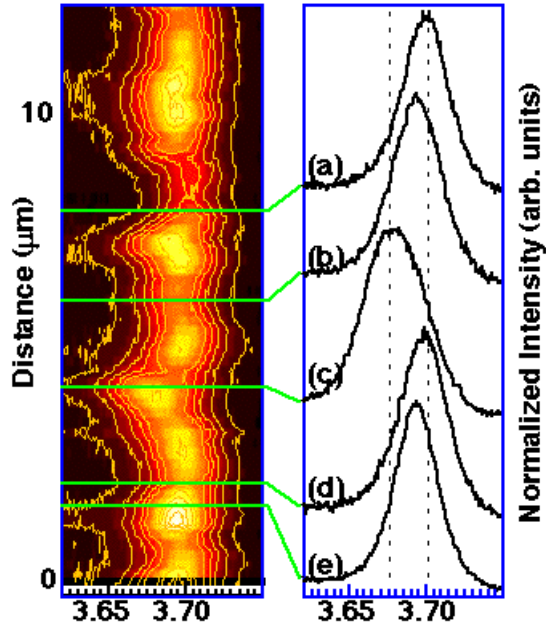


Figure 7. A series of cathodoluminescence spectra recorded in spot mode along a line on an AlGaIn film.

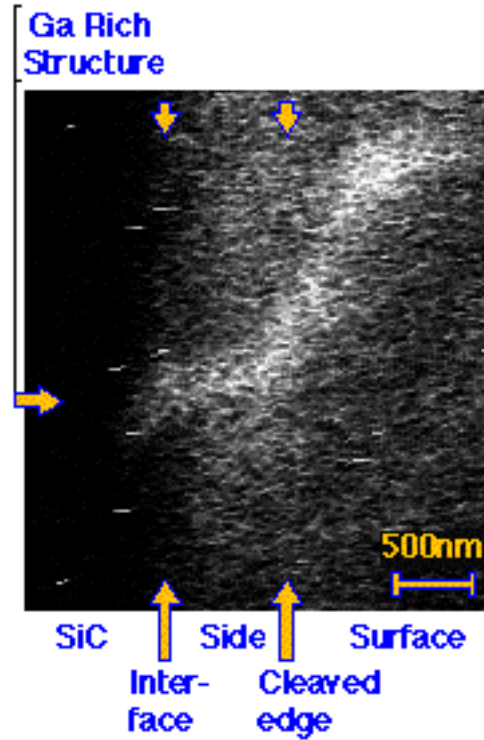


Figure 9. Monochromatic CL images from the cleaved edge of an AlGaIn epitaxial film, with the same mounting as the sample in figure 8

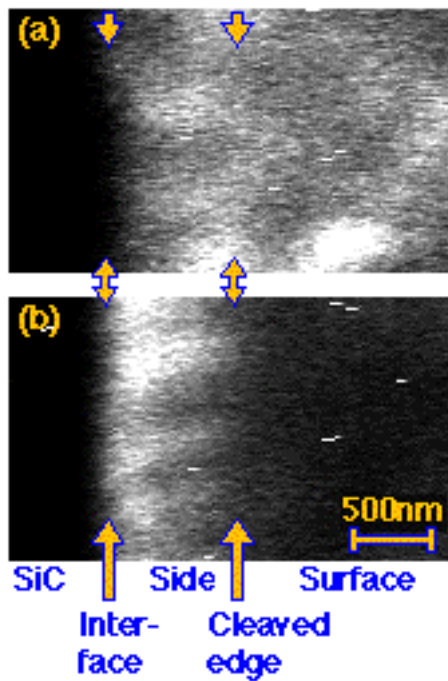


Figure 8. Monochromatic CL images from the cleaved edge of an AlGaIn epitaxial film. Recorded at (a) 3.69 eV and at (b) 3.75 eV. The sample was mounted with an approximate tilt of 45 degrees. The dark left part of the image is the SiC and the brighter region in the center of the image correspond to the side of the epitaxial film. The right part corresponds to the top of the epitaxial film.

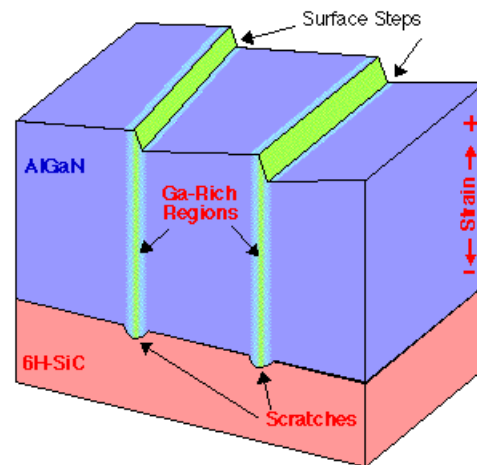


Figure 10. Schematic diagram of the model for the epitaxial AlGaIn film.